

# 1 Seasonal Rainfall Forecasts for the Yangtze River Basin 2 in the Extreme Summer of 2020

3 Philip E. BETT\*<sup>1</sup>, Gill M. MARTIN<sup>1</sup>, Nick DUNSTONE<sup>1</sup>, Adam A. SCAIFE<sup>1,2</sup>,  
4 Hazel E. THORNTON<sup>1</sup>, Chaofan LI<sup>3</sup>

5 <sup>1</sup>*Met Office Hadley Centre, FitzRoy Road, Exeter EX1 3PB, UK*

6 <sup>2</sup>*College of Engineering, Mathematics and Physical Sciences, University of Exeter,*  
7 *Exeter, EX4 4QF, UK*

8 <sup>3</sup>*Center for Monsoon System Research, Institute of Atmospheric Physics, Chinese*  
9 *Academy of Sciences, Beijing 100029, China*

## 10 ABSTRACT

11 Seasonal forecasts for Yangtze River basin rainfall in June, May–June–July (MJJ) and  
12 June–July–August (JJA) 2020 are presented, following successful forecasts in previous  
13 years. The 3-month forecasts are based on dynamical predictions of an East Asian Summer  
14 Monsoon (EASM) index, which is transformed into regional-mean rainfall through linear  
15 regression. The June rainfall forecasts for the middle/lower Yangtze River basin are based  
16 on linear regression of precipitation. The forecasts verify well in terms of giving strong,  
17 consistent predictions of above-average rainfall at lead times of at least 3 months. However,  
18 the Yangtze region was subject to exceptionally heavy rainfall throughout the summer  
19 period, leading to observed values that lie outside the 95% prediction intervals of the 3-  
20 month forecasts. Our forecasts are consistent with other studies of the 2020 EASM rainfall,  
21 whereby the enhanced Meiyu front in early summer is skilfully forecast, but the impact of  
22 mid-latitude drivers enhancing the rainfall in later summer is not captured. This case study  
23 demonstrates both the utility of probabilistic seasonal forecasts for the Yangtze region, but  
24 also potential limitations in anticipating complex extreme events driven by a combination  
25 of coincident factors.

26 **Key words:** seasonal forecasting, flood forecasting, Yangtze basin rainfall, East Asian  
27 Summer Monsoon.

## 28 Article Highlights:

- 29 ● Seasonal forecasts for Yangtze rainfall in June, MJJ and JJA 2020 are presented.  
30 ● The forecasts correctly predicted above-average rainfall with high confidence.

---

\*Corresponding author: Philip E. BETT

Email: [philip.bett@metoffice.gov.uk](mailto:philip.bett@metoffice.gov.uk) Twitter: [@pbett](https://twitter.com/pbett)

This preprint is © Crown Copyright 2021 Met Office. It has been submitted *Adv. Atmos. Sci.* but has not yet been peer reviewed.

- 31 ● The observed values lie outside the 95% prediction interval of the 3-month forecasts.
- 32 ● This partial success is consistent with the event being driven by teleconnections from  
33 multiple sources, not all of which were predicted.

## 34 **1. Introduction**

35 The UK Met Office, in conjunction with colleagues in China, has been producing  
36 seasonal forecasts of summer rainfall in the Yangtze River Basin since 2016. Forecasts for  
37 the summer period are produced from late winter into spring, and delivered to the China  
38 Meteorological Administration (CMA) each month to help inform their official forecast  
39 messages to users across China. Development of these forecasts grew out of research  
40 demonstrating significant forecast skill in the region from the Met Office GloSea5 seasonal  
41 forecast system (Li et al., 2016) and the identification of a clear user requirement (Golding  
42 et al., 2017a), and they have continued each year following positive feedback (Golding et  
43 al., 2019). The initial trial in 2016 followed the strong El Niño event in winter 2015–2016,  
44 which provided a clear driver for likely flood conditions the following summer. The  
45 forecasts predicted a high likelihood of above-average rainfall in the May–June–July (MJJ)  
46 period, and closer to average conditions in June–July–August (JJA). These were borne out  
47 by the observations (Wang et al., 2017; Yuan et al., 2017; Bett et al., 2018), and the forecast  
48 trial was run again in summer 2017 and 2018 (Bett et al., 2020).

49 For the 2019 season, the forecast system was upgraded, following research on the use  
50 of an East Asian Summer Monsoon (EASM) index to skilfully forecast smaller, sub-basin  
51 regions (Liu et al., 2018). This linked with further research based on user evaluation of the  
52 earlier forecasts (Golding et al., 2017b), showing a clear requirement for improved spatial  
53 resolution and longer lead times (Golding et al., 2019). Thus, the forecasts issued in 2019  
54 and 2020 use an EASM index to give probabilistic predictions of mean rainfall in MJJ and  
55 JJA for the Upper and Middle/Lower Reaches of the Yangtze basin separately, as well as  
56 for the basin as a whole, from the preceding February. The 2019 forecasts gave good  
57 guidance for the modestly above-average conditions in MJJ 2019, and the near-normal  
58 conditions in JJA 2019 (Zeng et al., 2020; Bett et al., 2020).

59 For the 2020 season, the climate service was further extended to include forecasts of  
60 June mean rainfall in the Middle/Lower Reaches of the Yangtze basin. This was based on  
61 the demonstration of significant skill in GloSea5 for predicting June mean rainfall directly  
62 in this region (Martin et al., 2020), where much of the rainfall during June is contributed  
63 by the Meiyu rain band.

64 In this letter, we describe the forecasts produced for summer 2020, and how they  
65 compared to the subsequent observations. We briefly outline the forecast methodology and  
66 datasets used in section 2, before describing the forecast evolution and evaluation in section  
67 3. We summarise our results and discuss what we can learn from 2020 from a seasonal  
68 forecasting perspective in section 4.

## 69 **2. Data and methods**

70 Our Yangtze seasonal forecasts are produced using a hybrid statistical–dynamical  
71 method, designed to make the best use of the skill available in a seasonal climate prediction  
72 model, while also following a relatively straightforward approach that makes the forecast  
73 uncertainty clear, reliable and explicit to users.

74 The forecasts for MJJ and JJA are based on a seasonal mean forecast of the Wang &  
75 Fan (1999) East Asian Summer Monsoon (EASM) index, calculated from zonal wind at  
76 850 hPa,  $u_{850}$ , produced by the GloSea5 seasonal forecast system (MacLachlan et al.,  
77 2015). Liu et al. (2018) demonstrated that GloSea5 could forecast this index skilfully. The  
78 forecasts for June mean rainfall in the Middle/Lower Reaches of the Yangtze basin are  
79 based on the GloSea5 rainfall output for that month. The operational GloSea5 system  
80 running in 2020 used the Global Coupled 2 configuration of the HadGEM3 climate model,  
81 described in detail in Williams et al. (2015). Two forecast ensemble members are produced  
82 each day, and a full 42-member forecast ensemble can be constructed for a given start date  
83 by pooling together the runs from the three weeks prior to that date. A hindcast ensemble  
84 is produced alongside the forecasts for calibration, covering the 24 years 1993–2016. Seven  
85 hindcast ensemble members are produced on four fixed dates each month, and a full  
86 hindcast ensemble corresponding to a given forecast is assembled from the hindcast start  
87 dates closest to the forecast members’ start dates, as described in MacLachlan et al. (2015).

88 The EASM index is defined as the difference between the mean  $u_{850}$  in two boxes, one  
89 centred on the South China Sea minus one centred on the East China Sea (Bett et al., 2020),  
90 and is closely related to the West Pacific Subtropical High. Low values of the index  
91 correspond to anomalously anticyclonic circulation in the western North Pacific, acting to  
92 enhance the northward advection of moisture that occurs as part of the Meiyu front: this  
93 leads to increased rainfall in the Yangtze basin. High values of the EASM index on the  
94 other hand, corresponding to anomalously cyclonic circulation in the western North  
95 Pacific, act against this northward flow over China, resulting in less rainfall over the  
96 Yangtze, but more rainfall in southern China.

97 We use the linear regression between the hindcast ensemble-mean EASM index and  
98 the historical observed precipitation as the basis for calibrated forecasts for MJJ and JJA,  
99 and between the hindcast ensemble-mean and the observed mean precipitation for the June  
100 forecasts. We use data from the Global Precipitation Climatology Centre (GPCC,  
101 Schneider et al., 2011, 2015) as the observations. The linear regression is shown as a scatter  
102 plot in the issued forecasts, together with a contingency table describing the hit rate and  
103 false alarm rate for forecasts of above-average precipitation. (An example of a forecast  
104 document is provided as Supplementary Information.) This provides a very clear  
105 demonstration of both the skill and the uncertainty in the forecast: for example, while the  
106 linear regression shows that negative values of our EASM index often result in enhanced  
107 rainfall, the uncertainty shows that this outcome is of course is not guaranteed.

108 A probabilistic forecast is then produced by applying the linear regression to a new  
109 ensemble mean forecast value of the EASM index from GloSea5. The forecast central  
110 estimate is given by the regression line itself, with the forecast uncertainty given by the  
111 prediction interval on the regression. This method automatically bias-corrects for the mean

112 and variance, and calibrates the forecast probabilities (Bett et al., 2020), within the  
113 limitations given by the length of the hindcast data set.

114 Bett et al. (2020) demonstrated that rainfall in the Middle/Lower Reaches of the  
115 Yangtze basin can be skilfully predicted in this way for the MJJ period, and the Upper  
116 Reaches in JJA. These regions are defined in terms of the Yangtze watershed, divided in  
117 two by a line at  $111^{\circ}\text{E}$  (shown later in Figure 4). Bett et al. (2020) also showed there was  
118 skill for the whole basin average in both periods. In all cases, forecasts could skilfully be  
119 produced at lead times of at least 3 months, i.e. from February for MJJ, and from March  
120 for JJA. Martin et al. (2020) demonstrated that June mean rainfall in a box over the  
121 Middle/Lower reaches of the Yangtze basin ( $25^{\circ}$ – $32.5^{\circ}\text{N}$ ,  $110^{\circ}$ – $120^{\circ}\text{E}$ ) can be skilfully  
122 predicted directly by GloSea5 from February onwards, a lead time of 4 months.

123 Operationally, forecasts were produced every Sunday from February to June for  
124 internal monitoring. They were issued to CMA in the first week of each month, on 4<sup>th</sup>  
125 February, 3<sup>rd</sup> March, 1<sup>st</sup> April and 4<sup>th</sup> May (produced on the Sundays 2<sup>nd</sup> February, 1<sup>st</sup>  
126 March, 29<sup>th</sup> March, and 3<sup>rd</sup> May).

127 Finally, the observational rainfall data for summer 2020 were obtained from the GPCC  
128 monthly monitoring data set (Schneider et al., 2018).

### 129 **3. Forecasts and verification**

130 Figure 1 shows the evolution of the weekly forecasts of MJJ-mean rainfall in the  
131 Middle/Lower Reaches in 2020. The skill as measured by the correlation between hindcast  
132 and observations is consistently high (around 0.6), and the forecasts give consistently high  
133 probabilities of above-average rainfall in the region ( $>60\%$ ), irrespective of lead time. The  
134 probabilities of above-average rainfall increase as the lead time reduces, with the final  
135 forecast issued (end of March) having a probability of over 70% for above-average rainfall.  
136 However, Figure 1 also shows that the actual observed value from the GPCC data set is  
137 outside the 95% prediction interval of the forecast: the forecast central estimates remain  
138 within  $\pm 1\sigma$  of the historical observations, while the observed value of  $10.2 \text{ mm day}^{-1}$  is  
139  $\approx 3.5\sigma$  away from the 1993–2016 mean ( $6.5 \text{ mm day}^{-1}$ ). In fact, the 2020 observed value  
140 lies above the 99th percentile of the prediction interval distribution for the forecast issued  
141 on 1<sup>st</sup> April – i.e. a value this extreme would be highly unlikely to occur according to the  
142 forecast. Forecasts for the whole basin in MJJ show very similar behaviour (Figure 5 in the  
143 Appendix).

144 The corresponding results for the forecasts for the Upper Reaches in JJA are shown in  
145 Figure 2. The skill from the hindcast is lower in this case, although it remains statistically  
146 significant at the 5% level throughout. The forecast probability of above-average rainfall  
147 in the region is again  $>60\%$  at all lead times, and indeed rises to  $>80\%$  in the weeks after  
148 the final forecast was issued in early May. The skill also increased in this period, and the  
149 forecast central estimate reaches about  $+1\sigma$  above average. Nevertheless, the observed  
150 value,  $7.1 \text{ mm day}^{-1}$ , is over  $3.5\sigma$  above average, outside the 95% prediction intervals of  
151 the forecasts. Again, a similar pattern of behaviour is seen in JJA for the basin as a whole  
152 (Figure 6 in the Appendix).

153 Figure 3 shows the evolution of the weekly forecasts of June mean rainfall for the box  
154 covering the Middle/Lower Reaches in 2020. The skill is statistically significant at the 5%  
155 level for all forecasts until mid-April, and the forecasts give consistently high probabilities  
156 of above-average rainfall in the region (>60%) at all lead times from late February onwards.  
157 In contrast with the MJJ and JJA forecasts, the probabilities decrease from above 80% to  
158 just over 60% as the lead times reduce, returning to higher values for the final two forecasts  
159 in May. This is thought to be related to the increasing influence of less-predictable sub-  
160 seasonal variability on monthly mean rainfall predictions as the target month approaches,  
161 reducing the signal to noise ratio. In contrast with the MJJ and JJA forecasts, the actual  
162 observed value from the GPCP data set is within the 95% prediction interval of all the  
163 forecasts from March onwards.

164 The breakdown of the observations by month and season is shown in Figure 4. There  
165 are strong above-average anomalies in the Upper Reaches in all four months, and in the  
166 Middle/Lower Reaches in June and July. Outside the Yangtze Basin itself, it is clear that  
167 there was also heavy rainfall in north-eastern China in May, and again in August; and in  
168 southern China in July and August.

169 The latitudinal progression of the monsoon rainband (Meiyu) exhibited some  
170 particular features in summer 2020, which can be seen in Figure 4 but have been  
171 investigated in detail by Liu et al. (2020): Initially, the Meiyu rainband moves north from  
172 May to June, such that the June average map shows the peak rainfall lying north of the  
173 Yangtze River itself. However, in July, the rainfall peak shifted southwards again, and can  
174 be seen lying on the Yangtze River in our figure. In August the rainband returned to its  
175 usual progression north of the Yangtze basin. Clearly, this remarkable temporary reversal  
176 in the usual monsoonal flow in July contributed significantly to the extremely high net  
177 rainfall totals over the Yangtze basin in 2020.

#### 178 **4. Discussion and conclusions**

179 The rainfall in China throughout summer 2020 was truly exceptional, resulting in  
180 heavy flooding, and significant pressures on water control infrastructures such as the large  
181 hydroelectric dams along the Yangtze River. The seasonal forecasts for rainfall in June,  
182 MJJ and JJA 2020 described here provided good advice in terms of warning of the  
183 enhanced risk of above-average rainfall for both the Upper and Middle/Lower Reaches of  
184 the basin, as well as for the basin overall, at lead times of up to 3–4 months.

185 However, the 3-month forecasts, based on the EASM index, under-predicted the  
186 magnitude of the rainfall anomalies, and our model did not predict 2020 to be an  
187 exceptional year with respect to the 1993–2016 period (see the scatter plots in the forecast  
188 document attached as Supplementary Information). Li et al. (2021) have examined the  
189 wider behaviour of the GloSea5 forecast model data, and they demonstrate that the raw  
190 model precipitation forecasts gave anomalies of a similar magnitude, about  $1\sigma$ . They also  
191 showed that the sea surface temperature (SST) anomalies in the Indian Ocean and tropical  
192 Pacific were well forecast by GloSea5, leading to successful forecasts of the atmospheric  
193 circulation in the west north Pacific, as seen in the WPSH and characterised by our EASM  
194 index. This is consistent with Takaya et al. (2020), who showed how the 2019 extreme

195 positive Indian Ocean Dipole (IOD) event led to basin-wide Indian Ocean warmth by early  
196 summer 2020. Their forecasting experiments demonstrated that without this Indian Ocean  
197 warmth, the WPSH would have been weaker and there would have been much reduced  
198 Meiyu rainfall. However, the seasonal forecasting model they used (JMA/MRI-CPS2) also  
199 significantly underpredicted the rainfall anomaly, to a similar degree as GloSea5.

200 A consequence of GloSea5's successful forecasts of the EASM circulation is that our  
201 forecasts of June rainfall contained the observed value within their 95% prediction interval.  
202 Indeed, our targeting of June alone for 1-month forecasts is because of the high levels of  
203 skill originating in the EASM circulation (Martin et al., 2020). This also points towards the  
204 errors in the 3-month forecasts lying in the later summer.

205 Both Li et al. (2021) and Liu et al. (2020) identified a southward flow from north China  
206 towards the Yangtze basin, corresponding to the temporarily retreating Meiyu front in July  
207 (Liu et al. 2020) and the resulting extreme persistence in the Yangtze rainfall. Li et al.  
208 (2021) showed that this circulation feature was not forecast by GloSea5. Considering the  
209 June–July average, Li et al. (2021) related this southward flow to an intensification of the  
210 westerly jet stream over Asia, which GloSea5 was not able to reproduce. This is consistent  
211 with the investigation by Liu et al. (2020) on subseasonal timescales, which traced the  
212 phenomena further back to a period of negative anomalies in the summer North Atlantic  
213 Oscillation (NAO), occurring from late June and throughout July. They demonstrated that  
214 the ECMWF Extended Range Forecast model (i.e. on subseasonal timescales) was able to  
215 forecast the enhanced rainfall anomalies during the northward-advancing phase in the early  
216 summer, but was unable to capture the circulation features leading to the southward  
217 movement in July.

218 Although the teleconnection between the spring/summer NAO and the East Asian  
219 Summer Monsoon is well known (e.g. Linderholm et al., 2011; Bao-Qiang and Ke, 2012),  
220 this represents a problem for subseasonal and seasonal forecasts, as the summer NAO itself  
221 is not currently well predicted by models. Indeed, as emphasized by Liu et al. (2020), the  
222 most skilful forecast components are the tropical circulation, whereas the skill falls away  
223 when the midlatitude circulation becomes the dominant driver. One possibility might be to  
224 use SST patterns in the North Atlantic as an additional predictor in our forecasts, as it has  
225 been shown that these can drive the Eurasian wave patterns that modulate the EASM  
226 rainfall (e.g. Yuan et al., 2017; Li et al., 2018).

227 Our forecasts gave good warnings for above-average rainfall in the Yangtze basin in  
228 summer 2020, and particularly in June, based on successful forecasts of the East Asian  
229 Summer Monsoon circulation in the west north Pacific, as a correct response to the warm  
230 Indian Ocean (present in the initial conditions, but deriving ultimately from the extreme  
231 positive IOD event in autumn 2019). However, the forecast model failed to capture the  
232 midlatitude drivers that particularly affected the circulation in later summer, manifesting  
233 in changes in the East Asian Jet, which caused the Meiyu front to persist for longer over  
234 the basin resulting in the extreme rainfall and severe impacts. It is interesting that the  
235 forecast models used by Takaya et al. (2020) and Liu et al. (2020) seem to have similar  
236 drawbacks, as well as successes. It is clear therefore that further research is required to  
237 improve forecasts of extreme events driven by multiple climate factors.

238

239 **Acknowledgments.** This work and its contributors (Philip Bett, Gill Martin, Nick  
 240 Dunstone, Adam Scaife and Hazel Thornton) were supported by the UK-China Research  
 241 & Innovation Partnership Fund through the Met Office Climate Science for Service  
 242 Partnership (CSSP) China as part of the Newton Fund. Chaofan Li was supported by the  
 243 National Key Research and Development Program of China (2018YFC1506005) and  
 244 National Natural Science Foundation of China (41775083).

## 245 Appendix

246 Forecast timeseries for the whole Yangtze River Basin are presented here for MJJ  
 247 (Figure 5) and JJA (Figure 6).

248

249

## REFERENCES

250 Bao-Qiang, T and F. Ke, 2012: Relationship between the Late Spring NAO and Summer  
 251 Extreme Precipitation Frequency in the Middle and Lower Reaches of the Yangtze  
 252 River. *Atmos. Ocean. Sci. Lett.*, **5**, 455–460, [doi: 10.1080/16742834.2012.11447038](https://doi.org/10.1080/16742834.2012.11447038).

253 Bett, P. E., A. A. Scaife, C. Li, C. Hewitt, N. Golding, P. Zhang, N. Dunstone, D. M. Smith,  
 254 H. E. Thornton, R. Lu, and H-L. Ren, 2018: Seasonal Forecasts of the Summer 2016  
 255 Yangtze River Basin Rainfall. *Adv. Atmos. Sci.*, **35**, 918–926, [doi: 10.1007/s00376-  
 256 018-7210-y](https://doi.org/10.1007/s00376-018-7210-y).

257 Bett, P. E., N. Martin, A.A. Scaife, N. Dunstone, G. M. Martin, N. Golding, J. Camp, P.  
 258 Zhang, C. Hewitt, L. Hermanson, C. Li, H-L Ren, Y. Liu, and M. Liu, 2020: Seasonal  
 259 Rainfall Forecasts for the Yangtze River Basin of China in Summer 2019 from an  
 260 Improved Climate Service. *J. Meteorol. Res.* **34**, 904–916, [doi: 10.1007/s13351-020-  
 261 0049-z](https://doi.org/10.1007/s13351-020-0049-z).

262 Golding, N., C. Hewitt, P. Zhang, P. Bett, X. Fang, H. Hu, and S. Nobert, 2017a: Improving  
 263 user engagement and uptake of climate services in China. *Climate Services*, **5**, 39–45,  
 264 [doi: 10.1016/j.cliser.2017.03.004](https://doi.org/10.1016/j.cliser.2017.03.004).

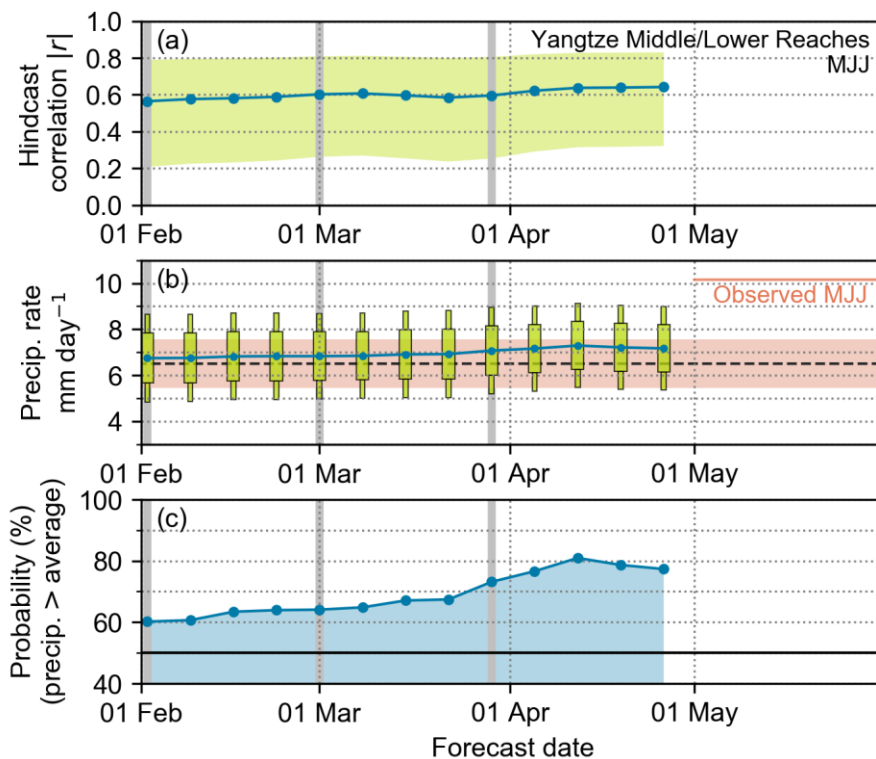
265 Golding, N., C. Hewitt, and P. Zhang, 2017b: Effective engagement for climate services:  
 266 Methods in practice in China. *Climate Services*, **8**, 72–76,  
 267 [doi: 10.1016/j.cliser.2017.11.002](https://doi.org/10.1016/j.cliser.2017.11.002).

268 Golding, N., C. Hewitt, P. Zhang, M. Liu, J. Zhang, and P. Bett, 2019: Co-development of  
 269 a seasonal rainfall forecast service: Supporting flood risk management for the Yangtze  
 270 River basin. *Climate Risk Management*, **23**, 43–49, [doi: 10.1016/j.crm.2019.01.002](https://doi.org/10.1016/j.crm.2019.01.002).

271 Li, C., A. A. Scaife, R. Lu, A. Arribas, A. Brookshaw, R. E Comer, J. Li, C. MacLachlan  
 272 and P. Wu, 2016: Skillful seasonal prediction of Yangtze river valley summer rainfall.  
 273 *Environ. Res. Lett.*, **11**, 094002, [doi: 10.1088/1748-9326/11/9/094002](https://doi.org/10.1088/1748-9326/11/9/094002).

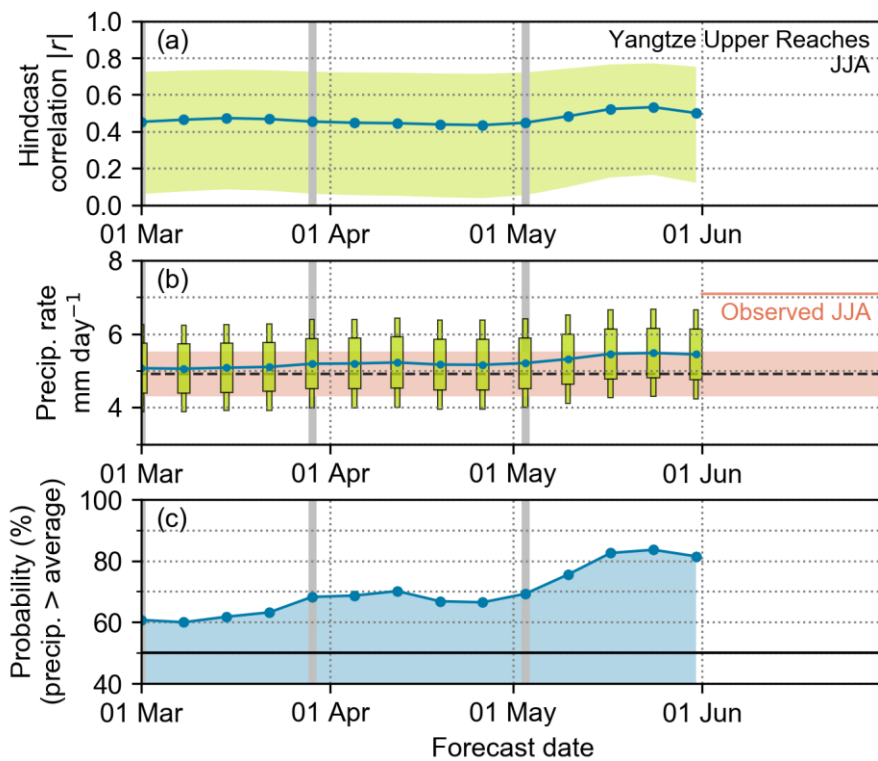
- 274 Li, C., R. Lu, N. Dunstone, A. A. Scaife, P. E. Bett, and F. Zheng, 2021: Seasonal  
275 prediction of the exceptional summer Yangtze River rainfall in 2020. Submitted to  
276 *Adv. Atmos. Sci.*
- 277 Li, W., H.-C. Ren, J. Zuo, H.-L. Ren, 2018: Early summer southern China rainfall  
278 variability and its oceanic drivers. *Clim. Dyn.*, **50**, 4691–4705, [doi: 10.1007/s00382-](https://doi.org/10.1007/s00382-017-3898-0)  
279 [017-3898-0](https://doi.org/10.1007/s00382-017-3898-0).
- 280 Linderholm, H. W., T. Ou, J.-H. Jeong, C. K. Folland, D. Gong, H. Liu, Y. Liu, and D.  
281 Chen, 2011: Interannual teleconnections between the summer North Atlantic  
282 Oscillation and the East Asian summer monsoon, *J. Geophys. Res.*, **116**, D13107,  
283 [doi: 10.1029/2010JD015235](https://doi.org/10.1029/2010JD015235).
- 284 Liu, B., Y. Yan, C. Zhu, S. Ma, and J. Li, 2020: Record-breaking Meiyu rainfall around  
285 the Yangtze River in 2020 regulated by the subseasonal phase transition of the North  
286 Atlantic Oscillation. *Geophys. Res. Lett.* **47**, e2020GL090342,  
287 [doi: 10.1029/2020GL090342](https://doi.org/10.1029/2020GL090342).
- 288 Liu, Y, H-L. Ren, A. A. Scaife, and C. Li, 2018: Evaluation and statistical downscaling of  
289 East Asian summer monsoon forecasting in BCC and MOHC seasonal prediction  
290 systems. *Quart. J. Roy. Meteor. Soc.*, **144**, 2798–2811, [doi: 10.1002/qj.3405](https://doi.org/10.1002/qj.3405).
- 291 MacLachlan, C., A. Arribas, K. A. Peterson, A. Maidens, D. Fereday, A. A. Scaife, M.  
292 Gordon, M. Vellinga, A. Williams, R. E. Comer, J. Camp, P. Xavier, and G. Madec,  
293 2015: Global Seasonal forecast system version 5 (GloSea5): a high-resolution seasonal  
294 forecast system. *Quart. J. Roy. Meteor. Soc.*, **141**, 1072–1084, [doi: 10.1002/qj.2396](https://doi.org/10.1002/qj.2396).
- 295 Martin, G. M., N. J. Dunstone, A. A. Scaife, and P. E. Bett, 2020: Predicting June Mean  
296 Rainfall in the Middle/Lower Yangtze River Basin. *Adv. Atmos. Sci.*, **37**, 29–41,  
297 [doi: 10.1007/s00376-019-9051-8](https://doi.org/10.1007/s00376-019-9051-8).
- 298 Schneider, U., A. Becker, P. Finger, A. Meyer-Christoffer, B. Rudolf, and M. Ziese, 2011:  
299 GPCP Monitoring Product: Near Real-Time Monthly Land-Surface Precipitation from  
300 Rain-Gauges based on SYNOP and CLIMAT data. Deutscher Wetterdienst (DWD),  
301 [doi: 10.5676/DWD\\_GPCP/MP\\_M\\_V4\\_100](https://doi.org/10.5676/DWD_GPCP/MP_M_V4_100).
- 302 Schneider, U., A. Becker, P. Finger, A. Meyer-Christoffer, B. Rudolf; and M. Ziese, 2015:  
303 GPCP Full Data Monthly Product Version 7.0 at 1.0°: Monthly Land-Surface  
304 Precipitation from Rain-Gauges built on GTS-based and Historic Data. Deutscher  
305 Wetterdienst (DWD), [doi: 10.5676/DWD\\_GPCP/FD\\_M\\_V7\\_100](https://doi.org/10.5676/DWD_GPCP/FD_M_V7_100).
- 306 Schneider, U., A. Becker, P. Finger, A. Meyer-Christoffer, and M. Ziese, 2018: GPCP  
307 Monitoring Product: Near Real-Time Monthly Land-Surface Precipitation from Rain-  
308 Gauges based on SYNOP and CLIMAT data. Deutscher Wetterdienst (DWD),  
309 [doi: 10.5676/DWD\\_GPCP/MP\\_M\\_V6\\_100](https://doi.org/10.5676/DWD_GPCP/MP_M_V6_100).
- 310 Schneider, U., A. Becker, P. Finger, E. Rustemeier, and M. Ziese, 2020: GPCP Full Data  
311 Monthly Product Version 2020 at 1.0°: Monthly Land-Surface Precipitation from

- 312 Rain-Gauges built on GTS-based and Historical Data. Deutscher Wetterdienst (DWD),  
313 [doi: 10.5676/DWD\\_GPCC/FD\\_M\\_V2020\\_100](https://doi.org/10.5676/DWD_GPCC/FD_M_V2020_100).
- 314 Takaya, Y., I. Ishikawa, C. Kobayashi, H. Endo, and T. Ose, 2020: Enhanced Meiyu–Baiu  
315 rainfall in early summer 2020: Aftermath of the 2019 super IOD event. *Geophys. Res.*  
316 *Lett.*, **47**, e2020GL090671, [doi: 10.1029/2020GL090671](https://doi.org/10.1029/2020GL090671).
- 317 Wang, B. and Z. Fan, 1999: Choice of South Asian Summer Monsoon Indices. *Bull. Amer.*  
318 *Meteor. Soc.*, **80**, 629–638, [doi: 10.1175/1520-](https://doi.org/10.1175/1520-0477(1999)080<0629:COSASM>2.0.CO;2)  
319 [0477\(1999\)080<0629:COSASM>2.0.CO;2](https://doi.org/10.1175/1520-0477(1999)080<0629:COSASM>2.0.CO;2).
- 320 Wang, B., J. Li, and Q. He, 2017: Variable and robust East Asian monsoon rainfall response  
321 to El Niño over the past 60 years (1957–2016). *Adv. Atmos. Sci.* **34**, 1235–1248,  
322 [doi: 10.1007/s00376-017-7016-3](https://doi.org/10.1007/s00376-017-7016-3)
- 323 Williams, K. D., C. M. Harris, A. Bodas-Salcedo, J. Camp, R. E. Comer, D. Copsey, D.  
324 Fereday, T. Graham, R. Hill, T. Hinton, P. Hyder, S. Ineson, G. Masato, S. F. Milton,  
325 M. J. Roberts, D. P. Rowell, C. Sanchez, A. Shelly, B. Sinha, D. N. Walters, A. West,  
326 T. Woollings, and P. K. Xavier, 2015: The Met Office Global Coupled model 2.0 (GC2)  
327 configuration. *Geosci. Model Dev.*, **8**, 1509–1524, [doi:10.5194/gmd-8-1509-2015](https://doi.org/10.5194/gmd-8-1509-2015).
- 328 Yuan, Y., H. Gao, W. J. Li, Y. J. Liu, L. J. Chen, B. Zhou, and Y. H. Ding, 2017: The 2016  
329 summer floods in China and associated physical mechanisms: A comparison with 1998.  
330 *J. Meteor. Res.*, **31**, 261–277, [doi: 10.1007/s13351-017-6192-5](https://doi.org/10.1007/s13351-017-6192-5).
- 331 Zeng, H., C. Xiao, X. Chen, Y. Chen, and D. Ye, 2020: State of China’s climate in 2019.  
332 *Atmos. Oceanic Sci. Lett.*, **13**, 356–362, [doi: 10.1080/16742834.2020.1762159](https://doi.org/10.1080/16742834.2020.1762159).  
333



334  
 335  
 336  
 337  
 338  
 339  
 340  
 341  
 342  
 343  
 344

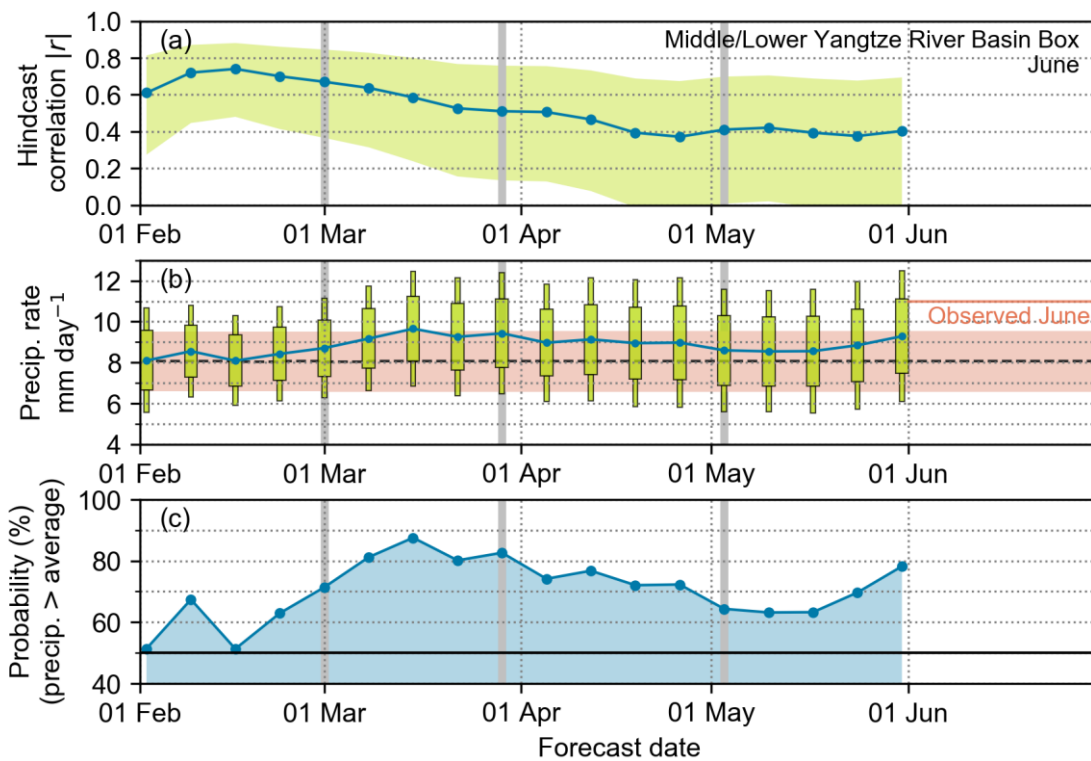
**Figure 1.** Forecasts for the Middle/Lower Reaches in MJJ 2020, as a function of lead time. The forecasts produced each week are shown as points, with grey vertical bars highlighting the monthly releases to CMA. Top (a): Absolute correlation between observations and the operational hindcasts available each week. The shading indicates the 95% confidence intervals on the correlation using a Fisher z test. Middle (b): The forecast signal from the linear regression, shown as the central estimates (blue line) and the 95% and 75% prediction intervals (green boxes). The observed mean over 1993–2016 is shown as a horizontal dashed line, with  $\pm 1$  standard deviation shown as orange shading. The observed value for MJJ 2020 is shown as a horizontal orange line from May. Bottom (c): The forecast probability of MJJ rainfall in this region being above the 1993–2016 average.



345

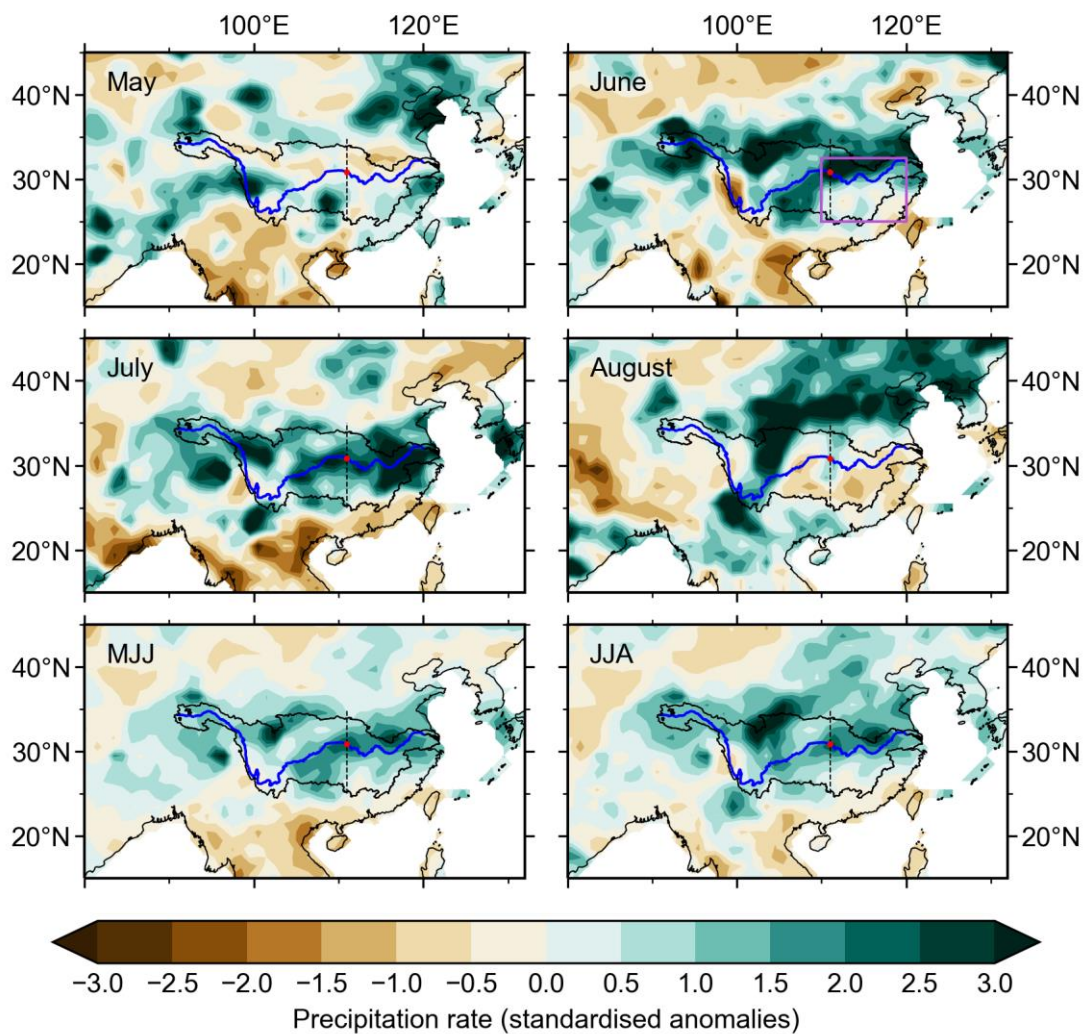
346 **Figure 2.** Forecasts for the Upper Reaches in JJA 2020, as a function of lead time, as in  
 347 Figure 1.

348



349

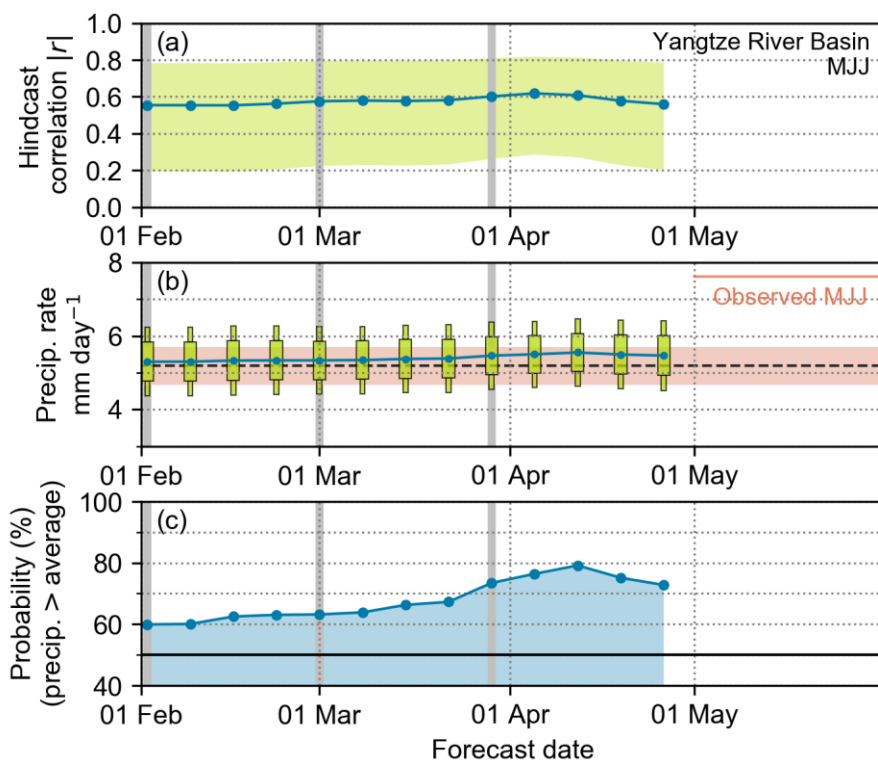
350 Figure 3. Forecasts for June 2020 mean rainfall in the box covering the Middle/Lower  
 351 Reaches ( $25^{\circ}$ – $32.5^{\circ}$ N,  $110^{\circ}$ – $120^{\circ}$ E), as a function of lead time, as in Figure 1.



352

353 **Figure 4.** Precipitation maps for summer 2020, based on GPCP monitoring data  
 354 (Schneider et al., 2018). Each month and season (see labels) are shown as standardized  
 355 anomalies with respect to their 1993–2016 mean and standard deviation from the latest  
 356 GPCP full data reanalysis (Schneider et al., 2020). The Yangtze River is marked in blue,  
 357 and the basin is outlined in black, with a black dashed line showing our separation into the  
 358 Upper Reaches and Middle/Lower Reaches. The box used for the Middle/Lower Reaches  
 359 forecasts in June is marked in purple on the June map. The location of the Three Gorges  
 360 Dam is marked in red.

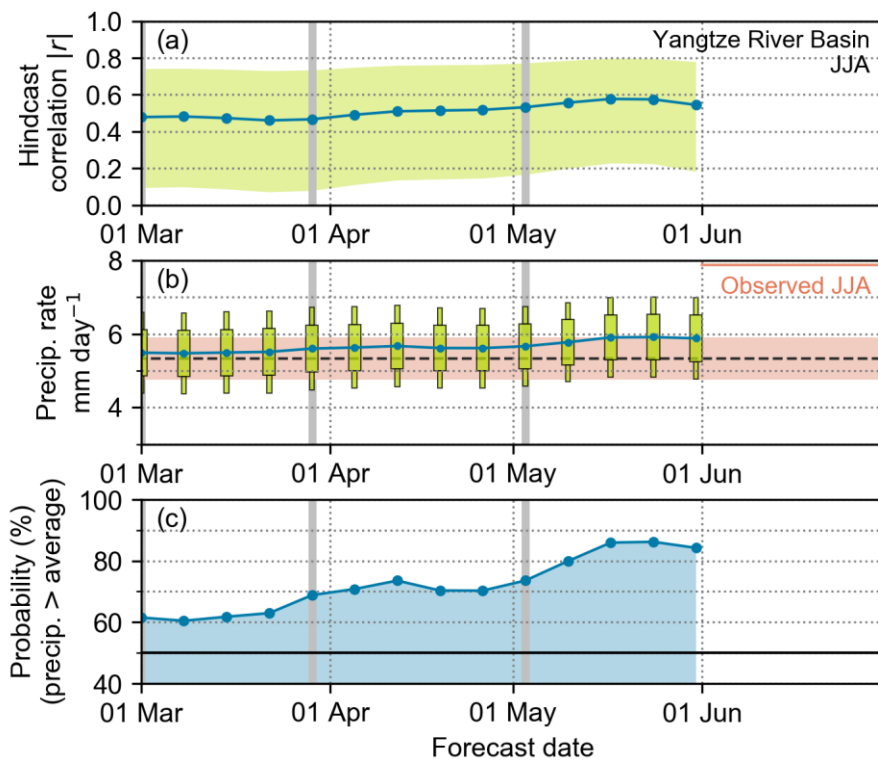
361



362

363 **Figure 5.** Forecasts for the whole Yangtze River Basin in MJJ 2020, as a function of lead  
 364 time, as in Figure 1.

365



366

367 **Figure 6.** Forecasts for the whole Yangtze River Basin in JJA 2020, as a function of lead  
 368 time, as in Figure 2.

369

370